Anhui Agricultural University

Comparative transcriptome and subcellular proteome analysis of *Bombyx mori* (Lepidoptera) larval midgut response to BmNPV in different resistant strains

Jiaping Xu, Ph D, Professor

Anhi Agricultural University, China

Introduction

The silkworm *Bombyx mori* L. (Lepidoptera: Bombycidae) has been domesticated for more than 5000 years and still plays an important role in many developing countries.

Bombyx mori nucleopolyhedrovirus (BmNPV) is a primary silkworm pathogen and annually causes serious economic losses.

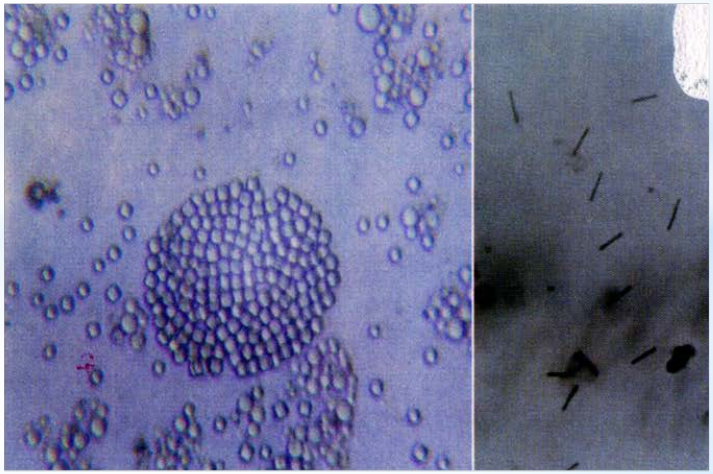

Silkworm midgut as the first barrier against pathogen infection

The midgut is not only the major tissue for food digestion but also an immune barrier against microorganism invasion and proliferation. Therefore, understanding the molecular mechanism of silkworm midgut response to BmNPV will help develop the novel strategy to control BmNPV.

- In recent years, Transcriptome sequencing was used widely in the research of host cell responses to exogenous pathogenic infection. For example, several candidate genes, such as *BmEts, BmToll10-3* and *Hsp20-1*, have been identified in the initial stage of BmNPV infection by analyzing the global transcriptional profile of silkworm cell lines following BmNPV infection (wang et al., 2015; Sagisaka et al., 2010).

The study of silkworm resistance to NPV infection at protein level

Many digestive enzymes involved in antiviral activity have been cloned and characterized, such as red fluorescent protein (RFP), lipase and serine protease.

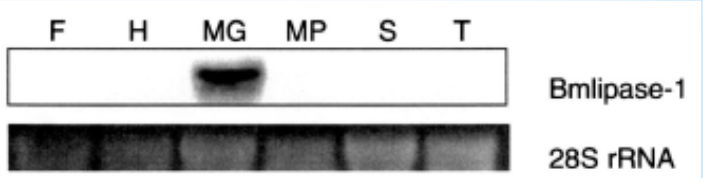

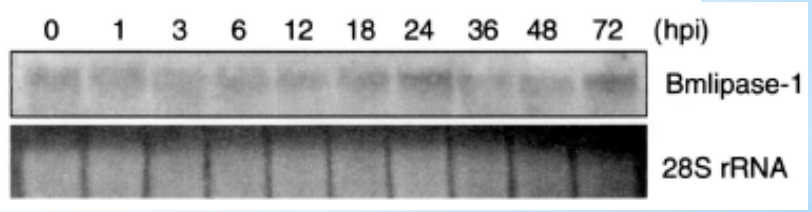

Ponnuvel *et al*., 2003

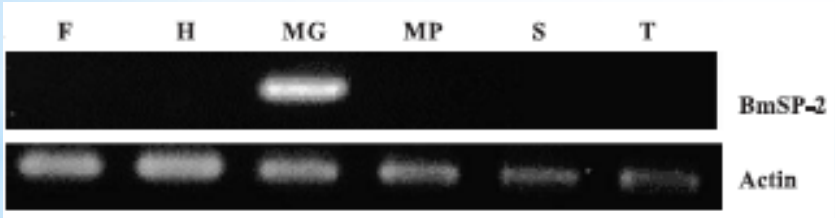

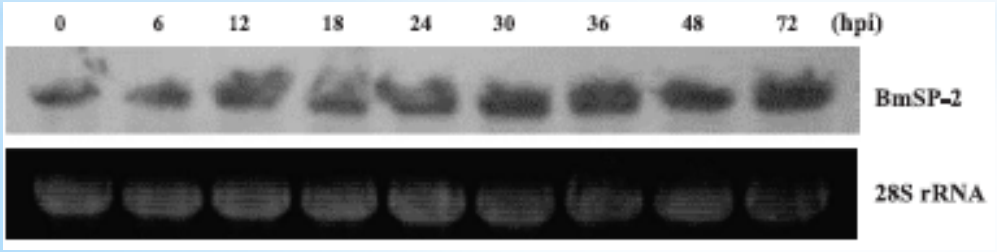

Hiroshi *et al*, 2004

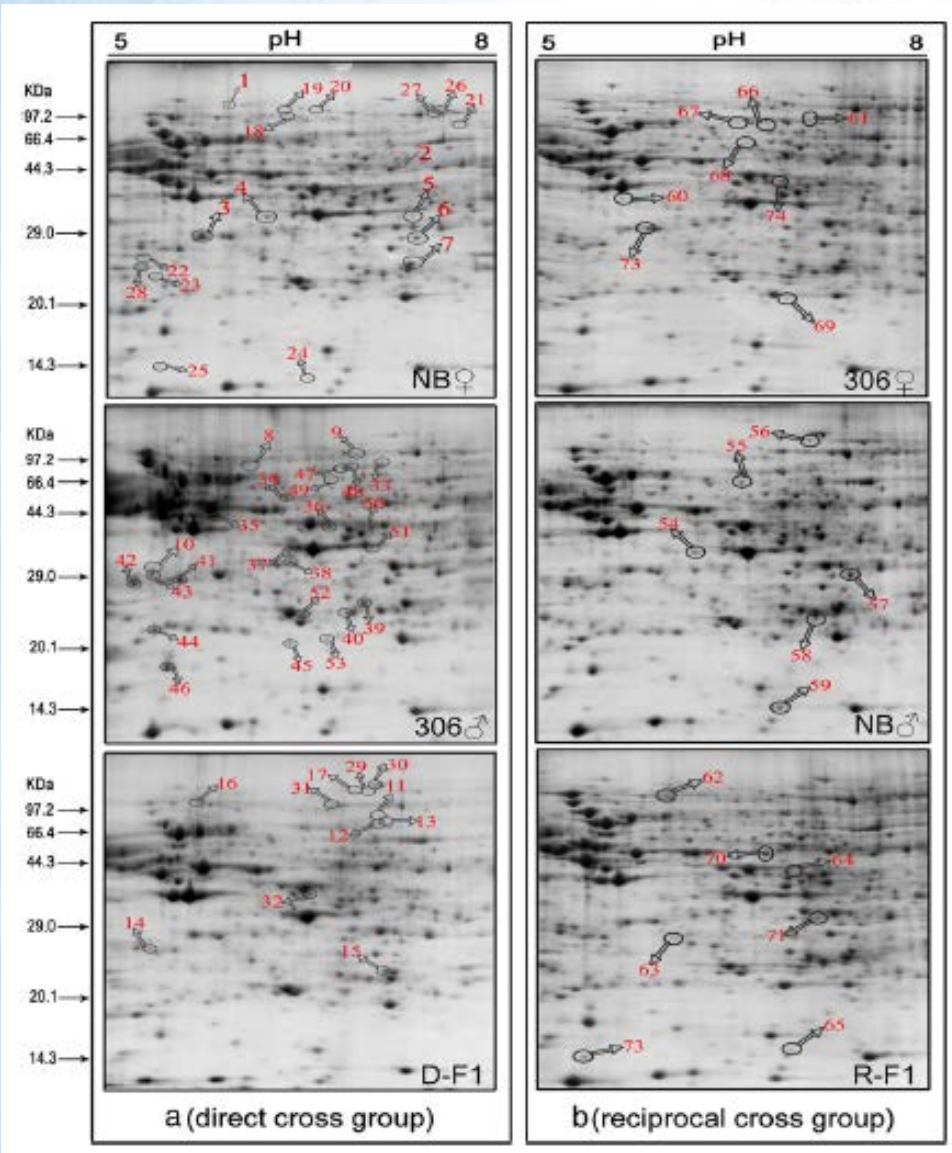

Qin *et al*., 2012

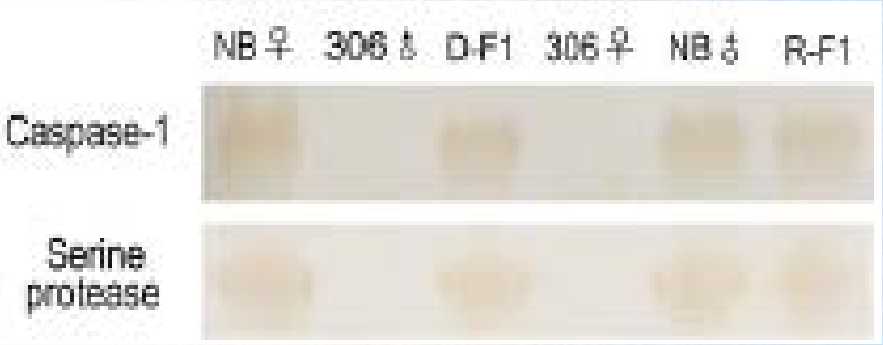

Caspase-1 and serine protease have been identified according to comparative proteomic analysis which might be involved in resistance to BmNPV.

- Recently, comparative subcellular proteomics has become a useful strategy to reduce sample complexity and protein overlapping in exploring disease-resistant mechanisms. Lu *et al.* (2016) has used the subcellular proteome to study the mechanism responsible for the Candidatus Liberibacter asiaticus-*Diaphorina citri* interactions.

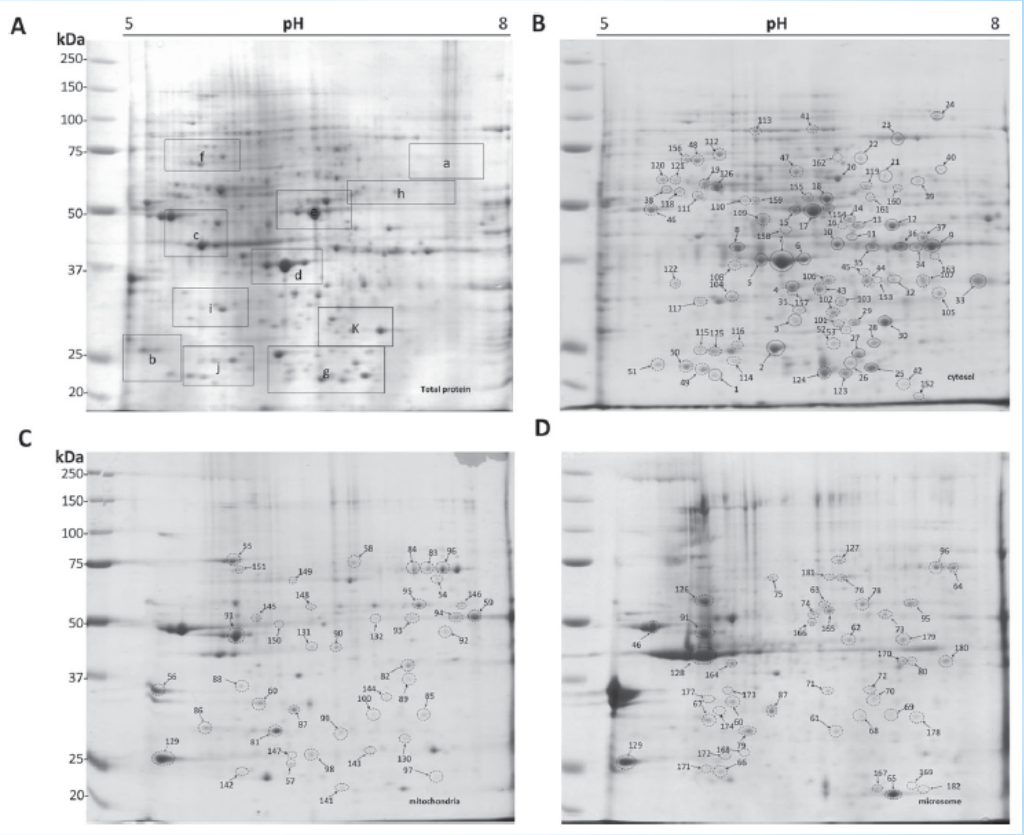

A, Total protein. B, Cytosol. C, Mitochondria. D, Microsome.

Lu *et al.*, 2016

- In our laboratory, 12 NPV binding proteins were obtained from silkworm midgut using 1D and 2-DE combined with Far-western.

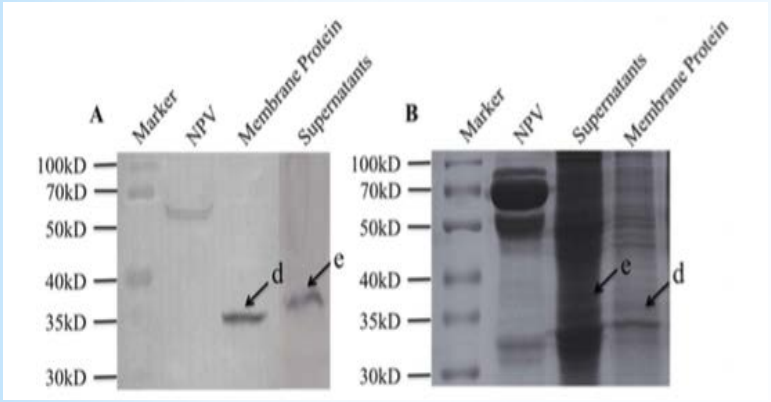

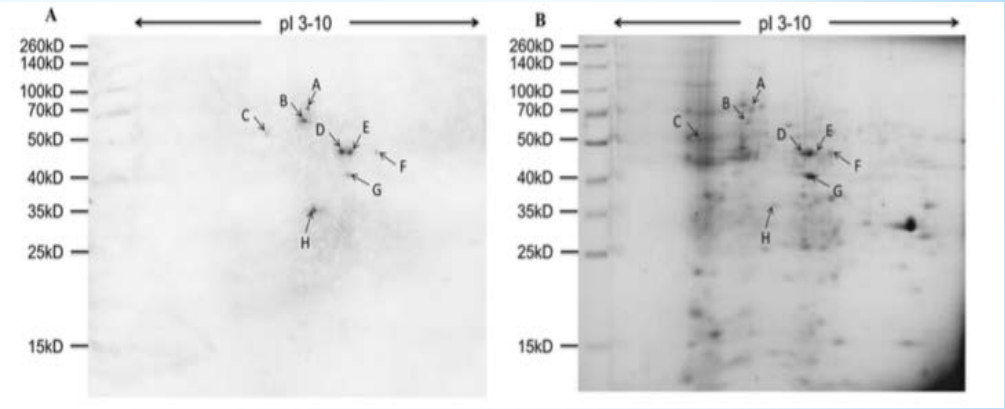

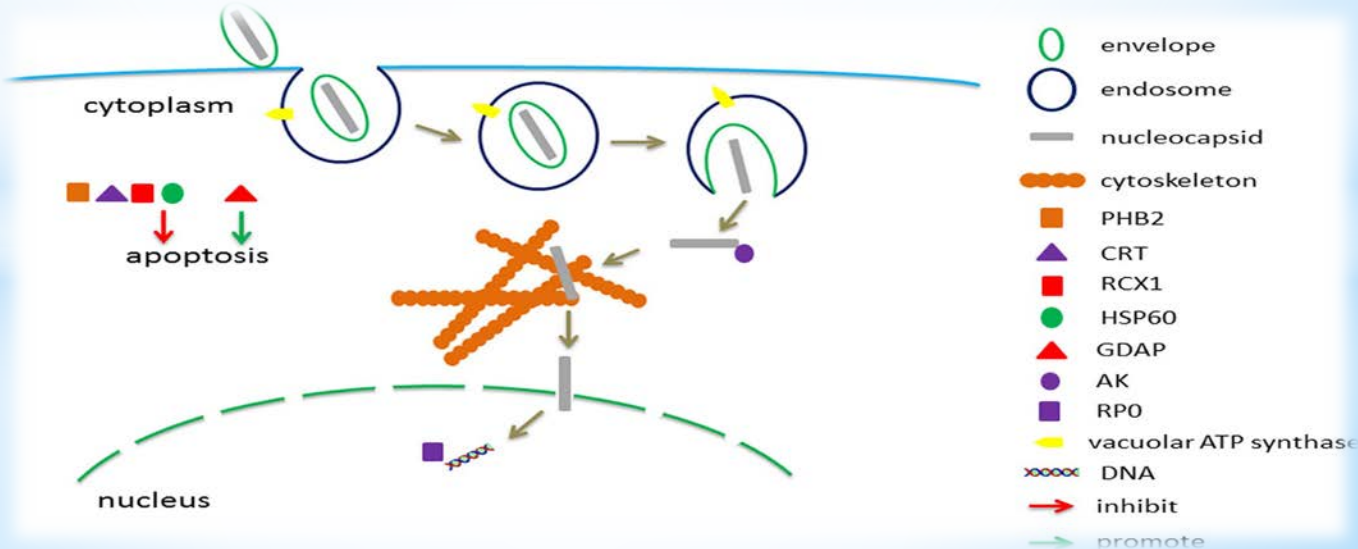

Cheng *et al*. 2015. PLOS ONE.

- Even though many remarkable results were obtained, the molecular mechanism of silkworm resistance to NPV infection was still unclear. Until now, the study of silkworm resistance to NPV infection using comparative transcriptome and proteome to analyze the near isogenic line and the backcrossed parent does not have been reported yet.

- In this study, comparative transcriptome and subcellular proteome were adopted to identify the differentially expressed genes and proteins in the near isogenic line BC9 and the backcrossed parent P50.

- The near-isogenic line was constructed by crossing recurrent parent to donor parent; progeny were repeatedly backcrossed with the recurrent parent for 9 generations. After several times backcrossing, the genetic background of near-isogenic line is very close to the recurrent parents.

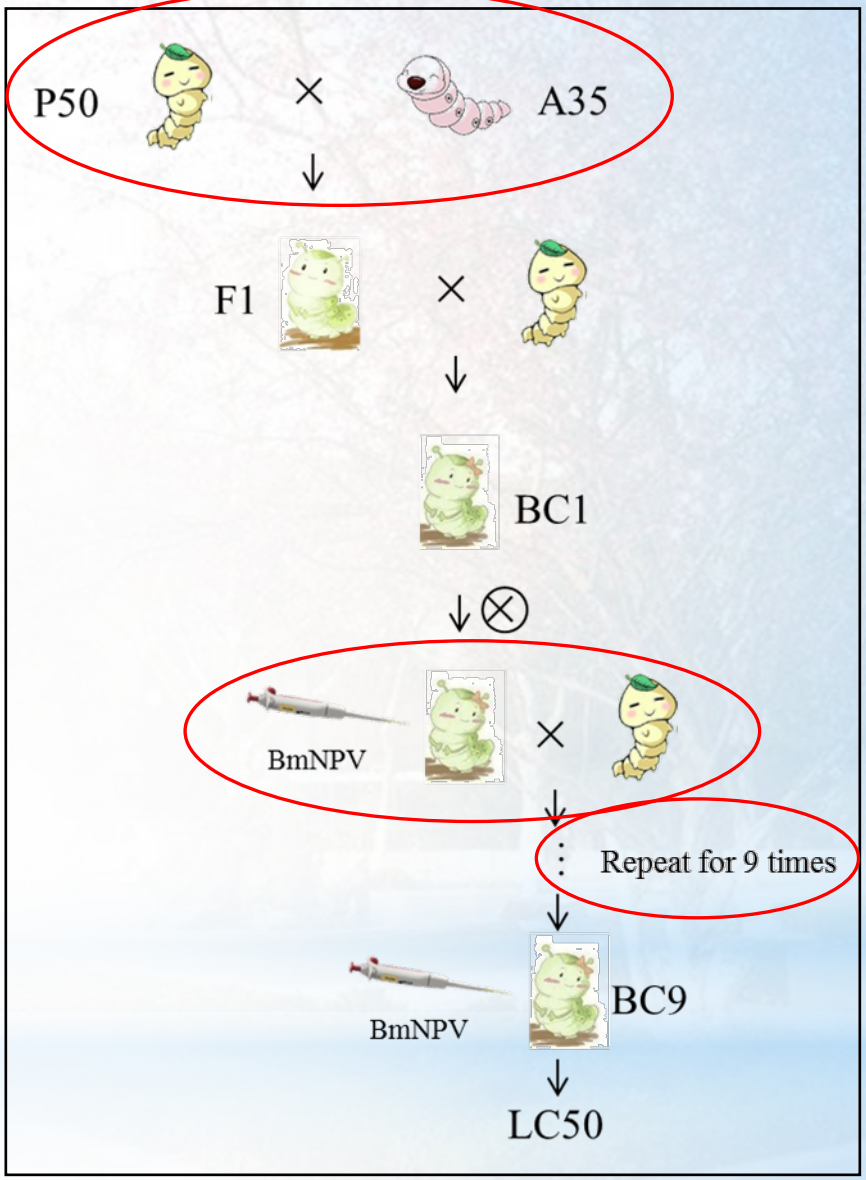

Construction of the near-isogenic BC9 strain

The LC_{50} value of *B. mori* larvae infected with BmNPV

Strains	LC50 (OB/mL)	95% fiducial limits	
		Lower	Upper
BC9	2.27×10^{6}	4.58×10^{5}	1.74×10^{7}
A35	5.90×10^{7}	2.14×10^{7}	3.22×10^{8}
P50	1.03×10^{5}	3.96×10^{4}	2.24×10^{5}

The LC_{50} value of A35 was 600-fold greater than that of P50.

The value of BC9 was 23-fold greater than that of P50.

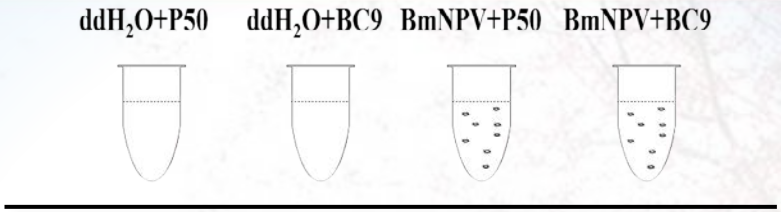

RNA-Seq

Data statistic

RT-qPCR

Reliability assessment

Screening of differentially expressed genes

GO analysis

Resistant genes

Protein metabolism

Cytoskeleton

Apoptosis

Further validation

Functional analysis

Mitochondria

Microsome

Cytosol

Subcellular fractions

2-DE

Screening of differentially expressed proteins

KEGG analysis

PPI analysis

RT-qPCR

I. Comparative Transcriptome Analysis of *Bombyx mori* (Lepidoptera) Larval Midgut Response to BmNPV in Susceptible and Near- Isogenic Resistant Strains

PLoS ONE, 2016

1. Summary statistics for silkworm genes based on the RNA-seq data.

	P50-	P50+	BC9-	BC9+
Total Reads	34,202,992	39,598,483	33,696,273	36,941,634
GC Content (%)	**48**	**49**	**48**	**48**
% ≥ Q30 (%)	**91.42**	**90.74**	**90.07**	**90.28**
Mapped Reads	27,261,542	31,333,514	26,640,096	29,131,867
Mapped Ratio (%)	**79.72**	**79.08**	**79.06**	**78.89**
Unique Mapped Reads	23,563,245	26,329,862	23,325,074	25,650,914
Unique Mapped Ratio (%)	68.90	66.51	69.21	69.47

The GC content of each of the four libraries was approximately 50%, and CycleQ30% was greater than 90% for each library.

All the unigenes matched previously described sequences with approximately 70% coverage.

Length distribution of unigenes in the assembled transcriptomes.

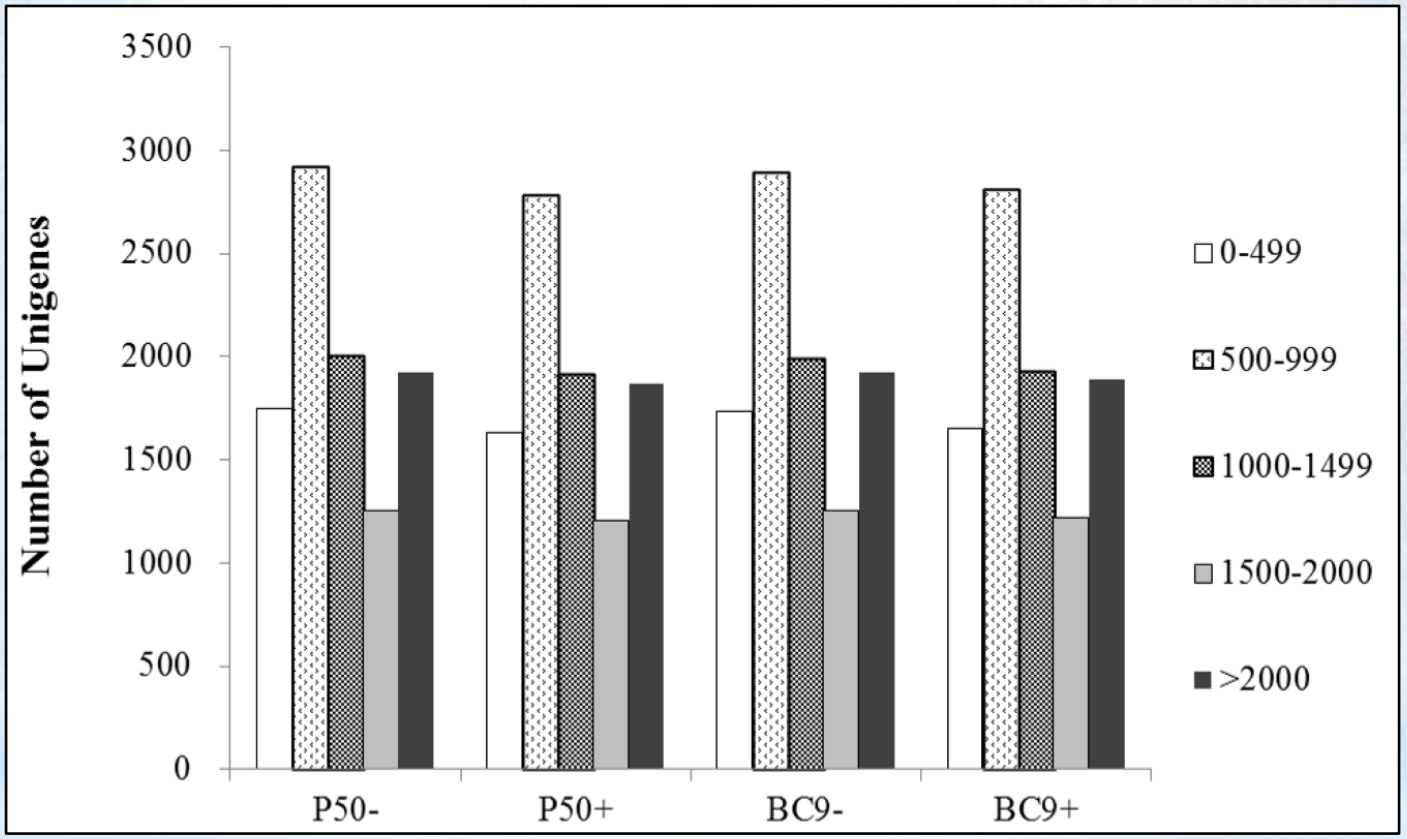

The length distribution of unigenes had similar patterns among the four libraries, suggesting that there was little bias in the construction of the four cDNA libraries

2. Correlation between gene expression ratios obtained from transcriptome data and RT-qPCR.

The relative expression levels of 15 randomly selected genes were analyzed by RT-qPCR. The results were consistent with the transcriptome data.

Linear regression analysis showed an R^2 value of 0.9169, which suggested a strong positive correlation between RT-qPCR and transcriptome data.

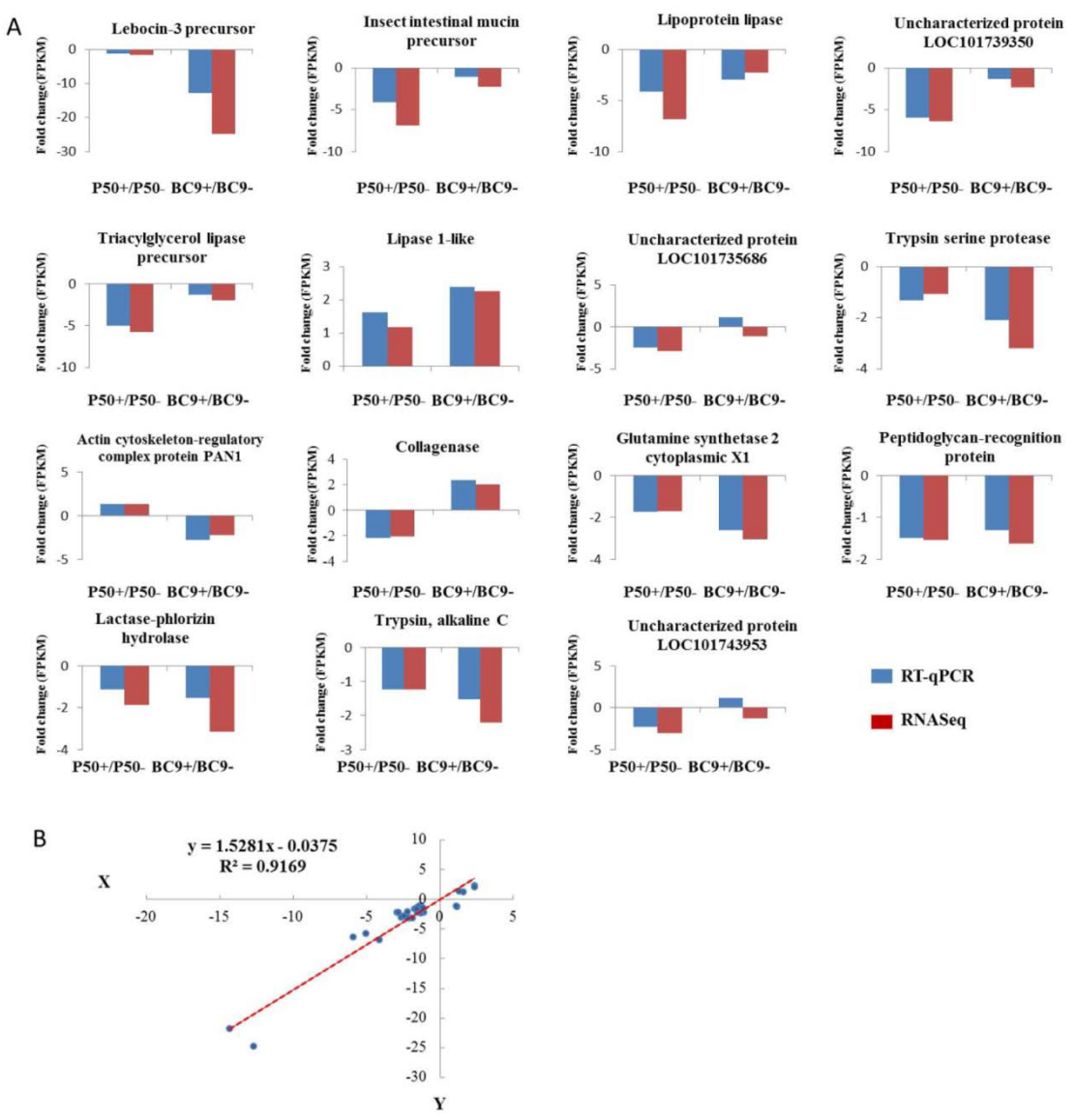

3. Venn diagram showing the DEGs related to BmNPV infection in different resistant strains.

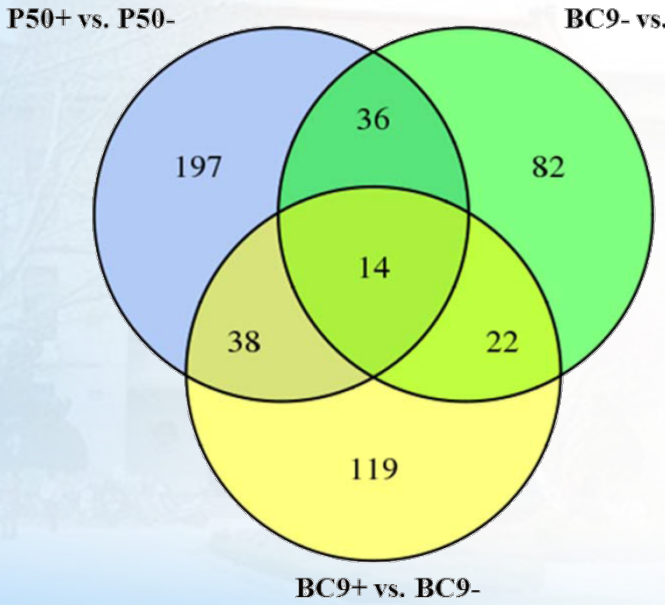

Groups	Total	Up-regulated	Down-regulated	Unique genes
P50+ vs. P50-	285	122 (43%)	163 (57%)	197
BC9+ vs. BC9-	193	56 (29%)	137 (71%)	119
BC9- vs. P50-	154	78 (51%)	76 (49%)	82

通过韦恩图分析，**197个基因**仅在**P50添毒前后表**现出差异表达，但上调和**下**调表达基因的数量没有明显的差异；同样的在两品系之间也并没有明显**的差异；但在BC9添毒前后的119差异表达基因中，71%的基因表**现出下调**表达。**

GO analysis

4. Gene ontology (GO) analysis of DEGs in different comparable groups.

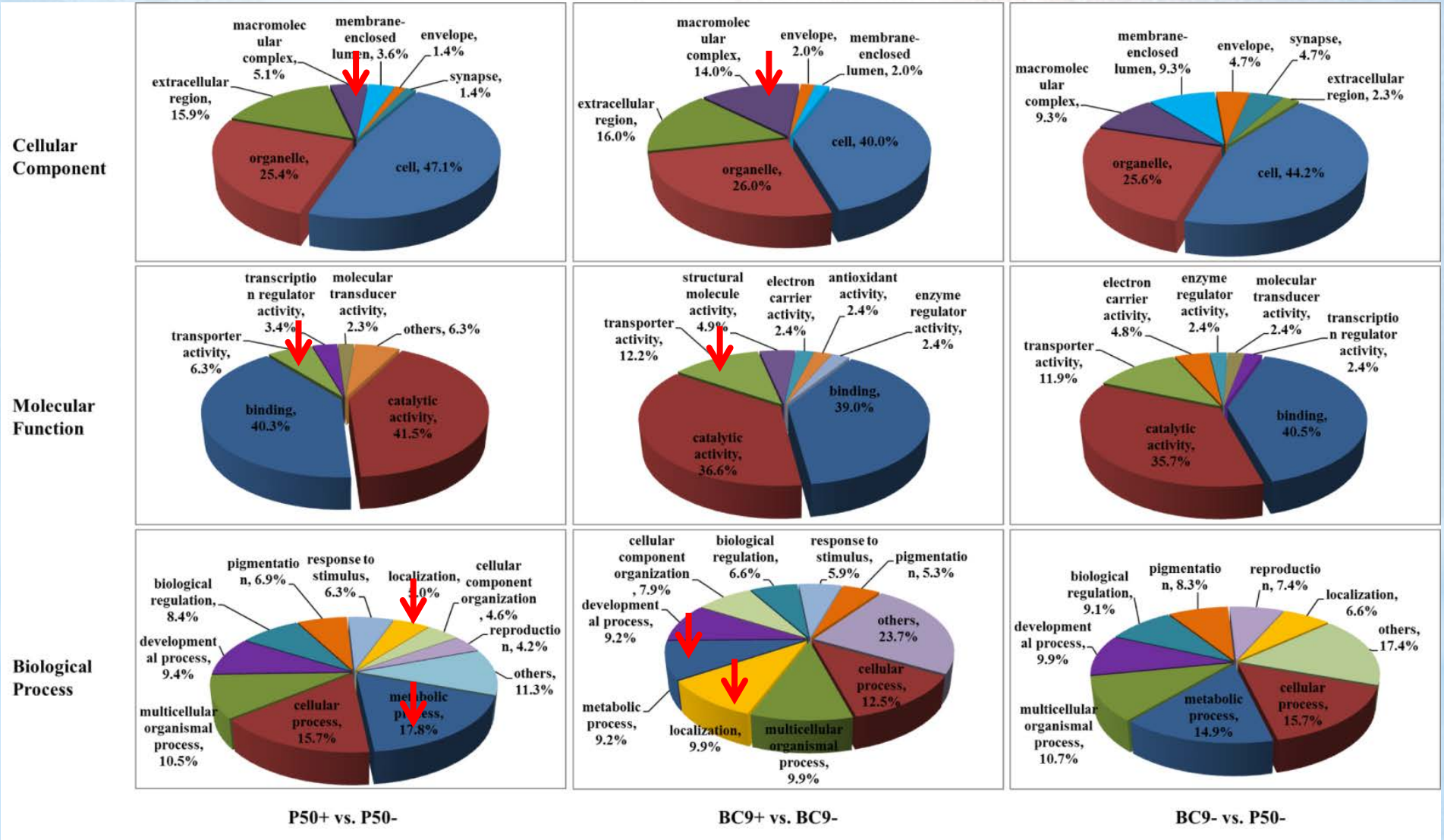

Identified differentially expressed genes involved in protein metabolism, cytoskeleton, and apoptosis related to BmNPV infection in different resistant strains.

Up-regulated
No difference
Down-regulated

Name	Gene ID	P50- FRKM	P50+ FPKM	BC9- FPKM	BC9+ FPKM	P50- vs. P50+ ratio	BC9- vs. BC9+ ratio
Protein metabolism							
Hypothetical protein KGM_08787	BGIBMGA003894	6.479	7.031	6.991	4.125	1.085	0.590
B(0,+)-type amino acid transporter 1	BGIBMGA007713	34.455	33.024	25.861	18.795	0.958	0.727
L-asparaginase	BGIBMGA012995	21.645	24.361	21.849	16.429	1.125	0.752
NEDD8-conjugating enzyme UBE2F	BGIBMGA013486	8.256	7.871	7.639	10.033	0.953	1.313
4-aminobutyrate aminotransferase	BGIBMGA006823	106.219	101.463	117.167	155.906	0.955	1.331
Uncharacterized protein LOC101742492	BGIBMGA006234	21.208	16.606	15.485	14.839	0.783	0.958
Proton-coupled amino acid transporter 4	BGIBMGA001151	1.715	3.412	2.198	1.239	1.990	0.564
Y+L amino acid transporter 2	BGIBMGA010801	1.541	2.816	2.030	1.249	1.827	0.615
Solute carrier family 12 member 6	BGIBMGA003629	1.068	1.736	0.867	0.564	1.625	0.651
Cystathionine gamma-lyase	BGIBMGA003656	219.509	270.108	184.300	138.484	1.231	0.751

80% ↑ 78% ↓

Up regulation

Up-regulated

No difference

Down-regulated

Name	Gene ID	P50- FRKM	P50+ FPKM	BC9- FPKM	BC9+ FPKM	P50- vs. P50+ ratio	BC9- vs. BC9+ ratio
Cytoskeleton							
Actin	BGIBMGA013945	945.736	1115.438	637.646	1057.763	1.179	1.659
Muscle LIM protein isoform 1	BGIBMGA001202	124.039	124.062	89.846	127.161	1.000	1.415
Apolipophorins isoform X2	BGIBMGA013341	2.345	3.642	2.198	2.856	1.553	1.300
Putative villin	BGIBMGA003119	6.824	6.585	7.700	9.502	0.965	1.234
Zinc finger protein Gfi-1b	BGIBMGA006132	12.448	18.952	12.387	9.220	1.522	0.744
Actin cytoskeleton-regulatory complex protein PAN1	BGIBMGA004121	83.016	99.504	54.242	28.428	1.199	0.524
Actin cytoskeleton-regulatory complex protein PAN1	BGIBMGA004002	4834.384	6342.360	4000.747	1781.384	1.312	0.445
Actin cytoskeleton-regulatory complex protein PAN1	BGIBMGA010768	7.855	45.723	7.668	0.250	5.821	0.033
Proteasomal ATPase-associated factor 1	BGIBMGA003545	4.920	8.102	6.756	7.861	1.647	1.164
Actin-binding protein	BGIBMGA013080	2.026	3.810	2.813	3.095	1.880	1.100
ATPase family AAA domain-containing protein 3	BGIBMGA000542	23.055	17.196	20.730	21.882	0.746	1.056

88% ↑ 50% ↓

Up-regulated

No difference

Down-regulated

Name	Gene ID	P50- FRKM	P50+ FPKM	BC9- FPKM	BC9+ FPKM	P50- vs. P50+ ratio	BC9- vs. BC9+ ratio
Apoptosis							
Conventional protein kinase C	BGIBMGA014132	0.352	0.305	0.384	0.250	0.866	0.652
Pyruvate dehydrogenase kinase	BGIBMGA003258	6.211	5.928	4.519	3.213	0.955	0.711
P53	BGIBMGA013185	0.714	0.687	0.675	0.552	0.963	0.818
Creb	BGIBMGA006865	21.657	21.099	23.179	18.966	0.974	0.818
Cytochrome c	BGIBMGA009012	1149.891	1072.848	1153.371	1464.034	0.933	1.269
Cell death activator CIDE-B	BGIBMGA011008	4.881	4.655	4.116	6.451	0.954	1.567
Caspase Nc	BGIBMGA002841	5.533	6.677	6.469	6.021	1.207	0.931
cAMP-dependent protein kinase C1	BGIBMGA011429	17.894	23.160	20.027	21.581	1.294	1.078
Tak1	BGIBMGA010752	6.565	8.039	6.933	7.573	1.224	1.092
Apoptosis-inducing factor	BGIBMGA014381	0.836	1.080	0.633	0.725	1.291	1.145
Protein kinase ASK1	BGIBMGA010545	1.928	2.558	2.321	2.588	1.327	1.115
Ribosomal protein S6 kinase, 90 kda	BGIBMGA011088	14.457	19.178	17.556	20.070	1.327	1.143
Daxx	BGIBMGA007470	7.205	9.653	9.246	9.842	1.340	1.065
TRAF6	BGIBMGA001290	1.493	2.077	1.604	1.906	1.392	1.188
TNFSF5	BGIBMGA003585	0.257	0.206	0.376	0.577	0.799	1.535
Survivin 2	BGIBMGA003946	0.521	0.387	0.585	1.015	0.743	1.737
App	BGIBMGA008317	0.075	0.032	0.045	0.093	0.433	2.059
Buffy	BGIBMGA001845	0.261	0.047	0.000	0.000	0.181	NA

67% ↑ 60% ↑

5. DEGs related to BmNPV infection in different resistant strains.

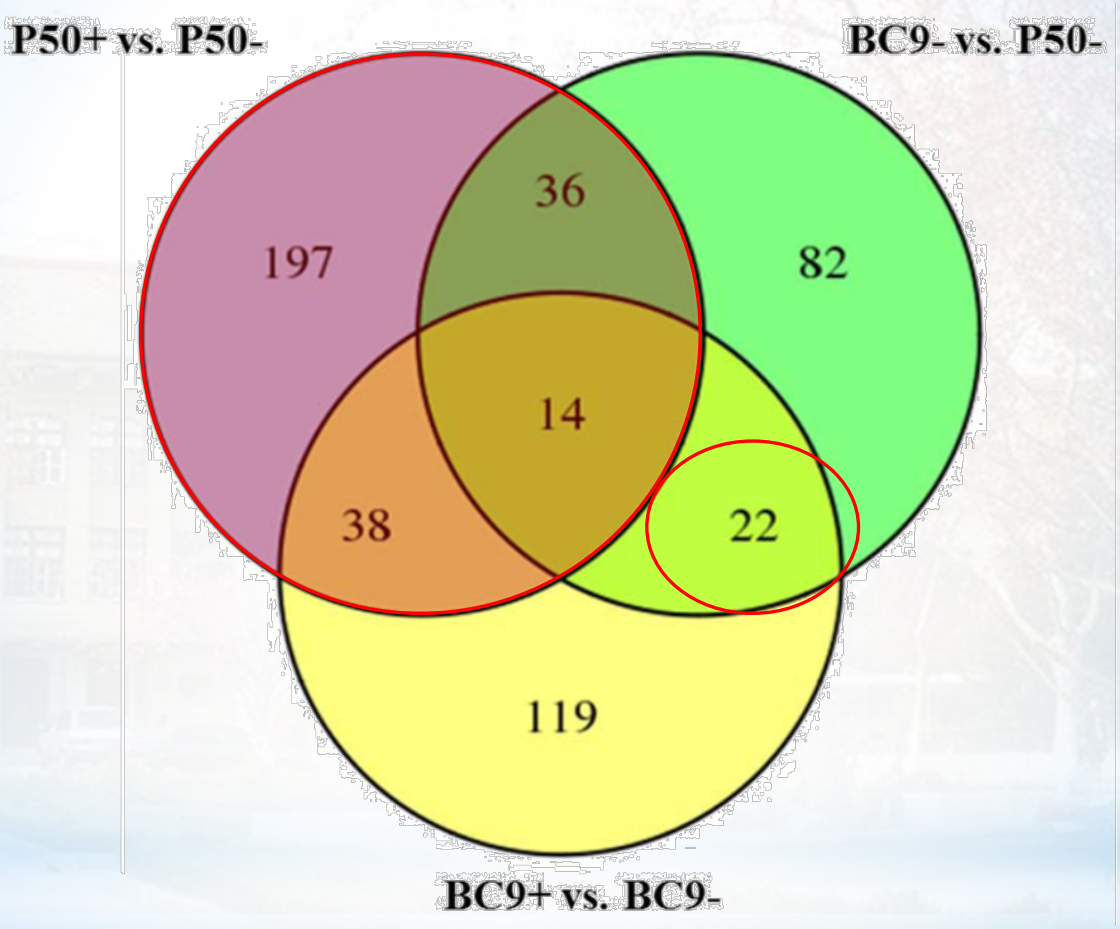

Venn diagram showing the DEGs related to BmNPV infection in different resistant strains.

22 genes was identified after removed genetic background and immune stress response.

Expression patterns of the 22 genes related to BmNPV resistance in different resistant strains.

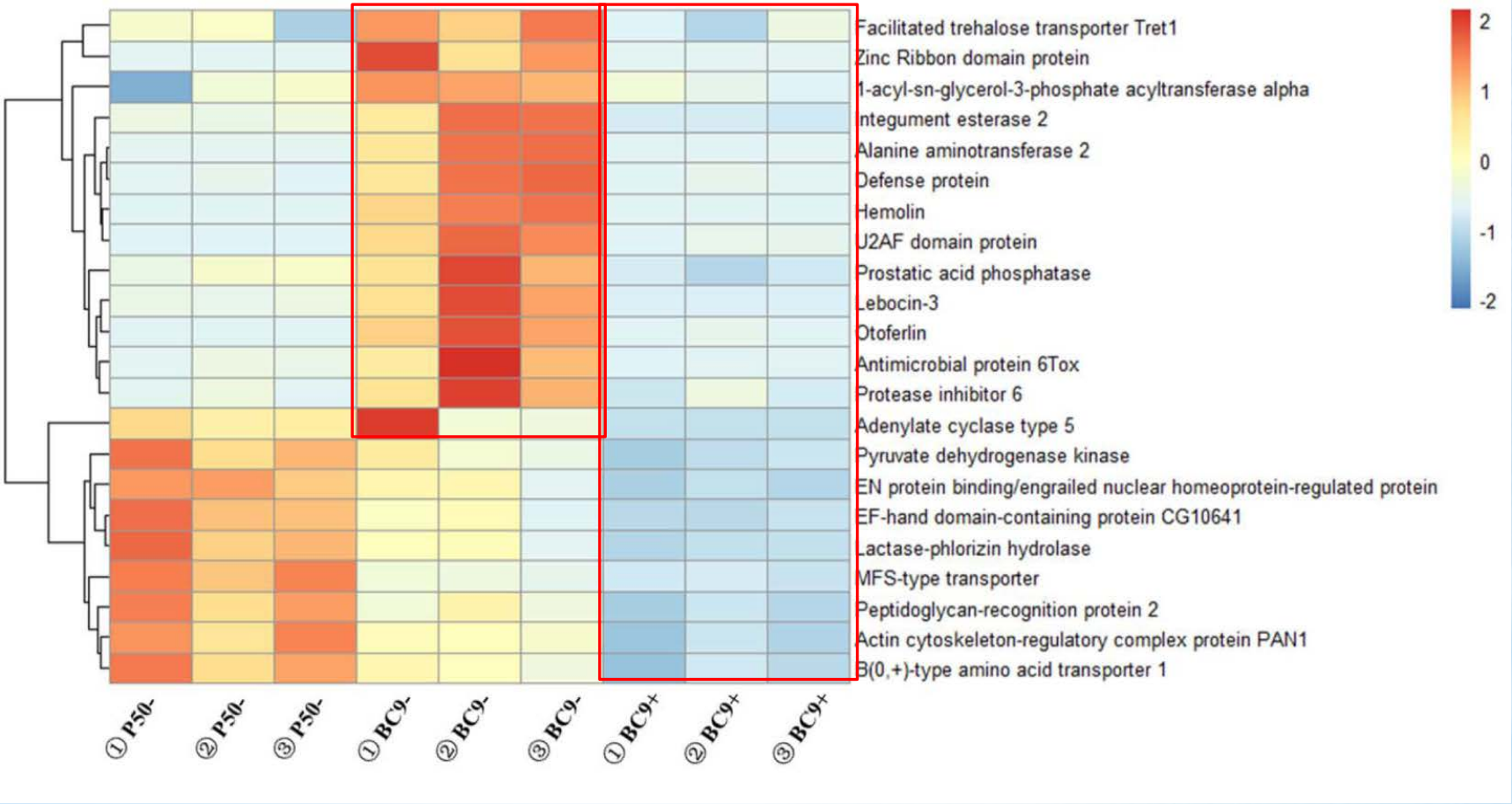

为了直观的反应这22个**基因的表达**谱，我们采用热图的方式进行呈现。结果可以**看出**这些基因在BC9**添毒后均表**现出下调。**在两品系之**间，13个基因在BC9中表现出上调。

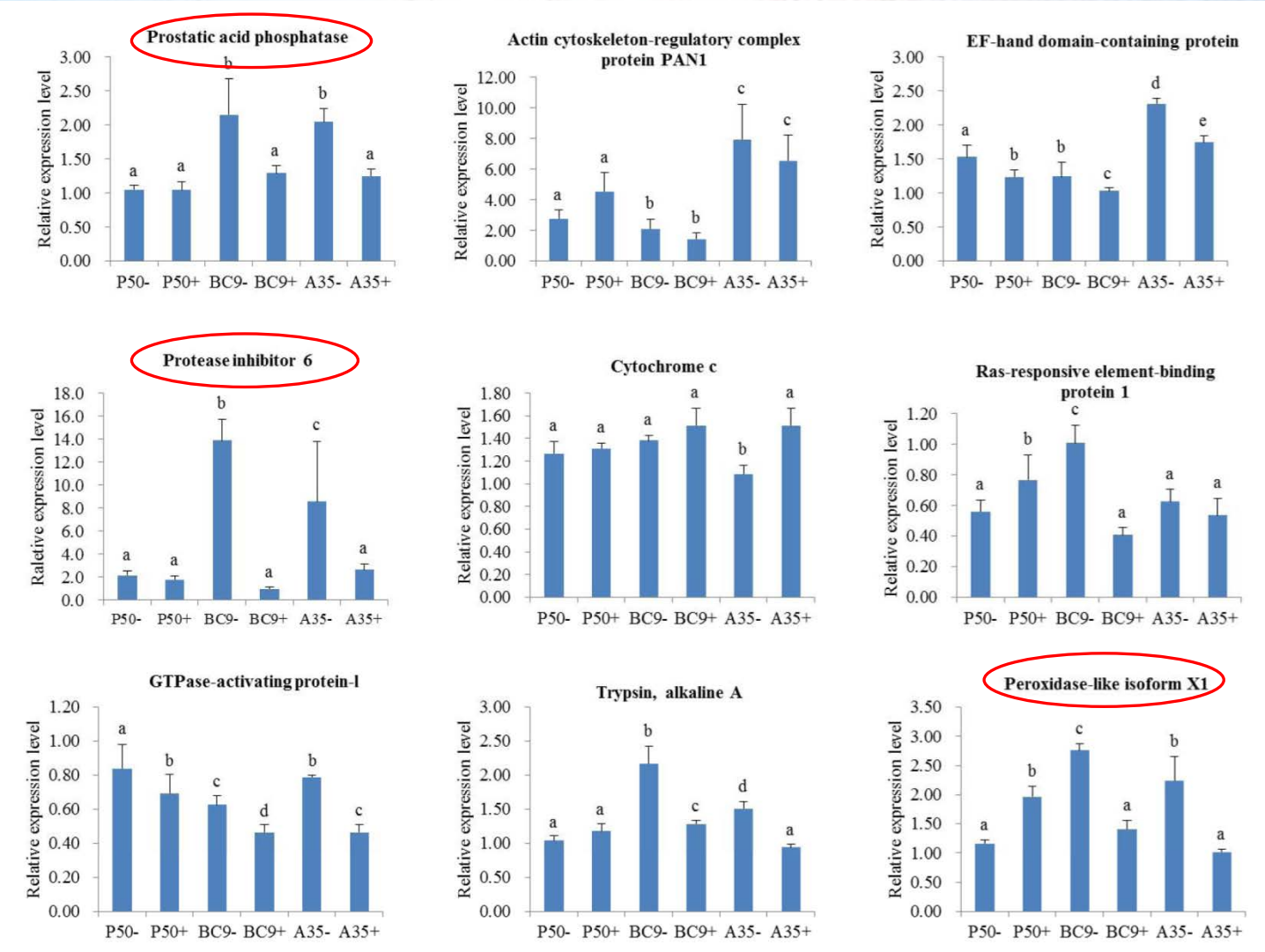

Real-time PCR analysis of expression profiles of resistant related genes in *B. mori* midgut.

5. Hypothesized modal analysis of the roles of the screened DEGs in BmNPV infection pathway.

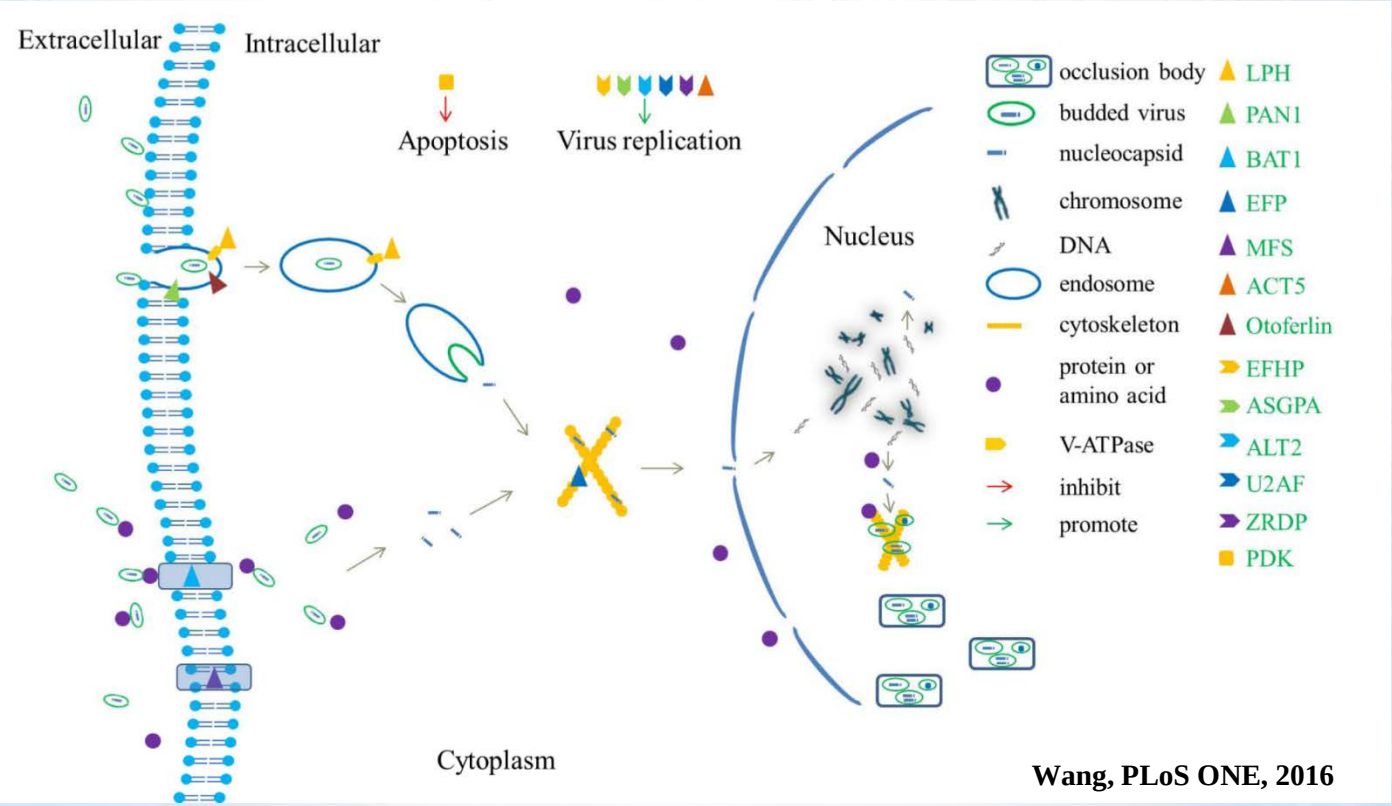

Wang, PLoS ONE, 2016

V-ATPase is activated by LPH to promote viral entry into the cytoplasm, a process which was also effected by PAN1 and Otoferlin. BAT1 related channel could serve as an alternative pathway for virus transmembrane transport. The released nucleocapsid is transported into the nucleus with the help of EFP. During replication, EFHP, ASGPA, ALT2, U2AF, ACT5 and ZRDP play an important role in facilitating virus replication. MFS is induced by the virus to increase cell volume leading to cell death. At the same time, the apoptosis process could be triggered by PDK to inhibit BmNPV infection.

II. Comparative Subcellular Proteomics Analysis of Susceptible and Near-isogenic Resistance *Bombyx mori* (Lepidoptera) Larval Midgut Response to BmNPV infection

Scientific Report, 2017

1. Analysis of subcellular protein fractions of silkworm midgut

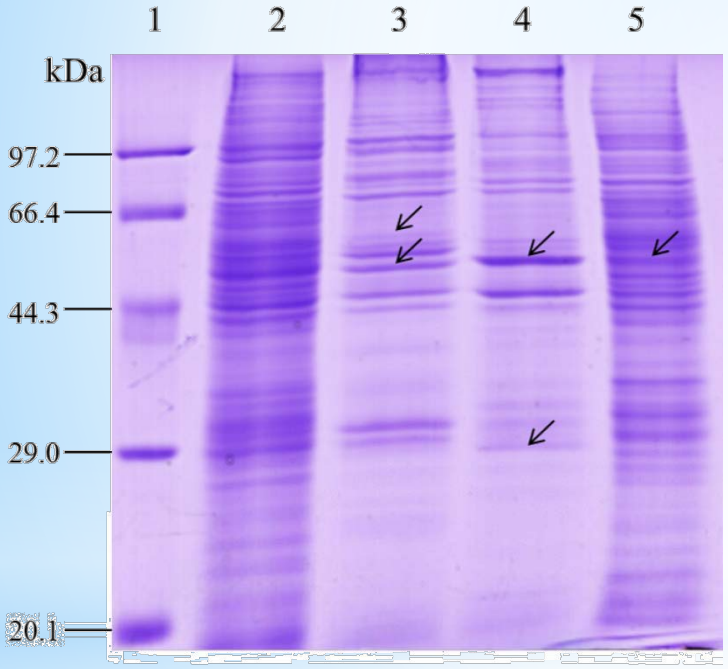

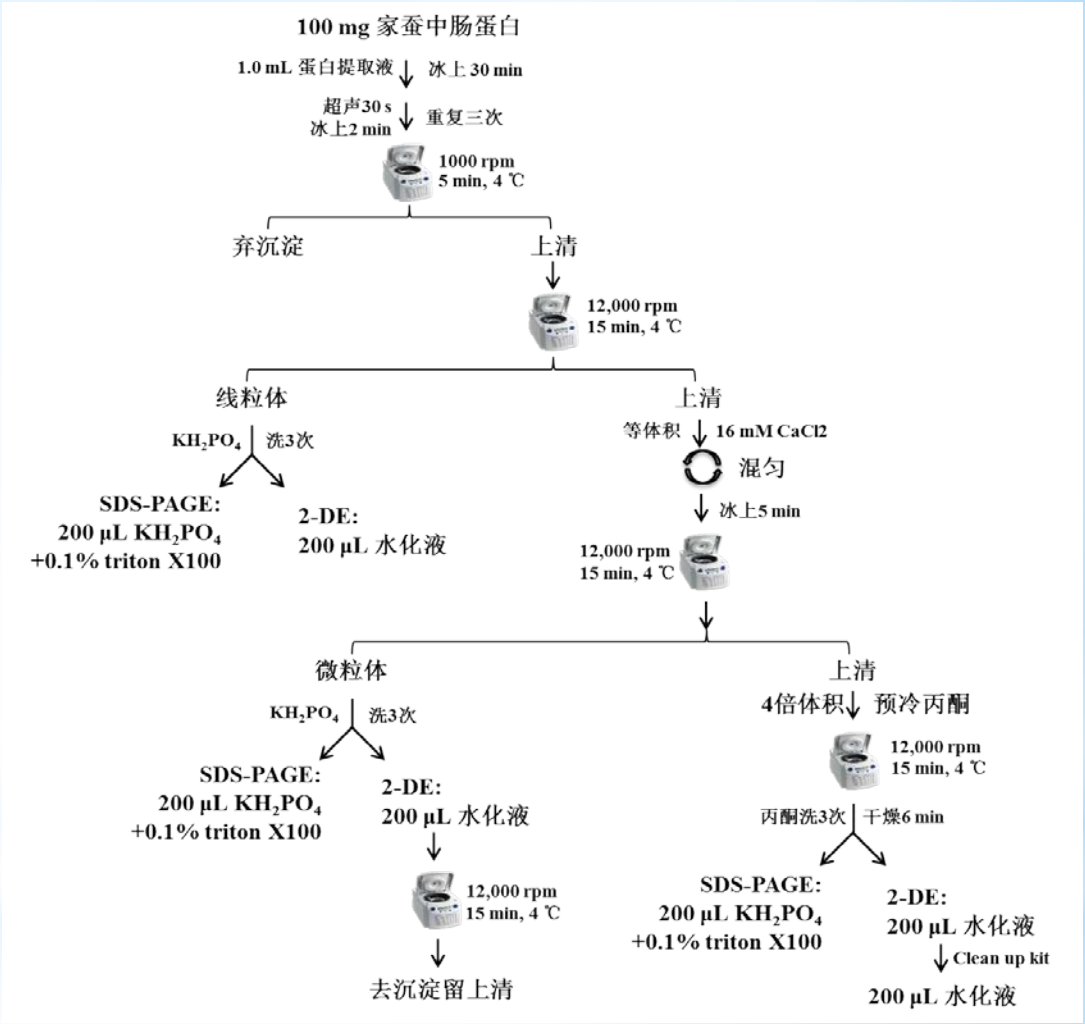

1, Marker; 2, total protein; 3, mitochondira; 4, microsome; 5, cytosol.

Subcellular protein resolution ratio is higher than total potiomics.

2. Cytosolic proteins

2-DE images of cytosolic protein extracts from P50 and BC9 following BmNPV infection.

A total of 38 DEPs in the cytosol with significant changes were selected for MALDI-TOF MS analysis.

Bio-Rad PDQuest software

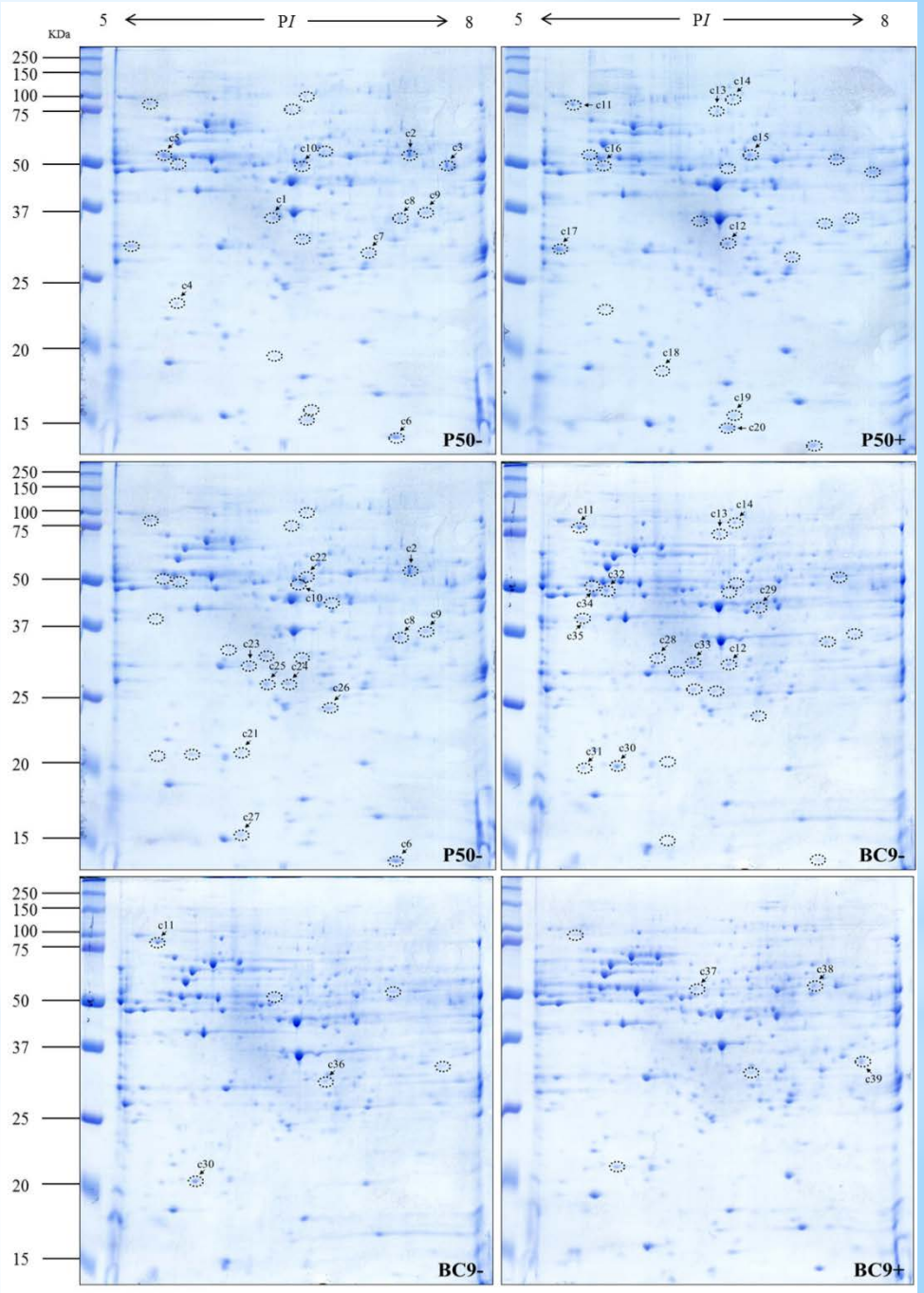

Identified proteins from cytosolic fraction that changed significantly in different resistant strains following BmNPV infection. MALDI-TOF MS

Spot no.[a]	P50+ vs. P50-[b]	Ratio[b]	Accession no.[c]	Protein name[c]	Theoretical/ Observed PI[d]	Theoretical/ Observed MW (kDa)[d]	Matched unique peptides[e]	Sequence coverage (%)[e]	Protein score[e]	Molecular/biological function[f]
c1	down	49.13	gi|255652881	Dnaj (Hsp40) homologue 3	5.56/6.47	40/35.25	6	23%	456	Protein folding
c2	down	65.71	gi|512914963	Probable methylmalonate-semialdehyde dehydrogenase [acylating], mitochondrial isoform X1	7.59/7.53	56/57	9	22%	808	Aldehyde dehydrogenase (NAD) activity, fatty-acyl-CoA binding, methylmalonate semialdehyde dehydrogenase (acylating) activity, thymine metabolic process, valine metabolic process
c3	down	149.67	gi|512936895	Acetyl-CoA hydrolase	7.67/7.83	52/48.4	8	16%	523	Hydrolase activity, acetyl-CoA metabolic process
c4	down	6.07	gi|512902782	Uncharacterized protein LOC101738880 isoform X1	5.75/5.72	25/22.73	7	34%	578	
c5	down	5.34	gi|17136564	Alpha-tubulin at 84B [Drosophila melanogaster]	5.00/5.62	51/53.44	8	27%	767	GTPase activity, GTP binding, structural constituent of cytoskeleton, antimicrobial humoral response, mitotic spindle assembly checkpoint
c6	down	2.4	gi|512934077	10 kDa heat shock protein, mitochondrial	6.74/7.38	11/15.22	4	52%	396	ATP binding, protein folding
c7	down	2.86	gi|827563568	Electron transfer flavoprotein subunit alpha, mitochondrial	8.43/7.2	35/29.68	8	36%	827	Electron carrier activity, flavin adenine dinucleotide binding
c8	down	3.72	gi|827558088	3-hydroxyisobutyryl-CoA hydrolase, mitochondrial	8.08/7.43	41/35.39	7	27%	584	Hydrolase activity
c9	down	8.15	gi|512898603	Glyoxylate reductase/hydroxypyruvate reductase-like isoform X1	8.76/7.65	40/36.95	10	33%	849	NAD binding, oxidoreductase activity, acting on the CH-OH group of donors, NAD or NADP as acceptor
c10	down	148.54	gi|112984390	Elongation factor 1-alpha	9.24/6.69	51/49.5	6	18%	390	GTPase activity, GTP binding, translation elongation factor activity
c11	up	3.09	gi|112983556	90-kDa heat shock protein	4.99/5.52	83/86.37	9	16%	713	ATP binding, response to stress, protein folding
c12	up	5.75	gi|512901366	Aldose reductase-like isoform X1	6.09/6.68	36/31.36	8	30%	491	Oxidoreductase activity
c13	up	4.58	gi|827560339	Prolyl endopeptidase	7.90/6.61	90/76.05	4	6%	309	Serine-type endopeptidase activity, serine-type exopeptidase activity
c14	up	3.66	gi|512888904	Cytoplasmic aconitate hydratase-like isoform X1	5.84/6.73	97/94.81	8	13%	55	Metabolic process
c15	up	5.93	gi|512939991	Cystathionine beta-synthase-like	6.02/6.86	54/54.31	8	18%	481	Cystathionine beta-synthase activity, metal ion binding, pyridoxal phosphate binding
c16	up	3.12	gi|357613322	26S protease regulatory subunit 6A [Danaus plexippus]	5.11/5.73	48/49.32	7	23%	493	ATP binding, peptidase activity, protein catabolic process
c17	up	3.14	gi|312597598	Inorganic pyrophosphatase	4.96/5.4	32/29.85	9	28%	452	Inorganic diphosphatase activity, magnesium ion binding, phosphate-containing compound metabolic process
c18	up	6.1	gi|512923641	Fatty acid-binding protein-like	5.04/6.16	16/18.89	5	38%	296	Lipid binding, transporter activity
c19	up	4	gi|512923641	Fatty acid-binding protein-like	5.04/6.7	16/16.44	5	33%	200	Lipid binding, transporter activity
c20	up	8.06	gi|512917297	Fatty acid-binding protein 1-like isoform X1	6.59/6.67	15/15.61	7	71%	573	Lipid binding, transporter activity

Spot no.[a]	BC9- vs. P50-[b]	Ratio[b]	Accession no.[c]	Protein name[c]	Theoretical/ Observed PI[d]	Theoretical/ Observed MW (kDa)[d]	Matched unique peptides[e]	Sequence coverage (%)[e]	Protein score[e]	Molecular/biological function[f]
c21	down	4.29	gi|512907055	Grpe protein homologue, mitochondrial	6.97/6.2	24/21.21	6	44%	491	Adenyl-nucleotide exchange factor activity, protein folding
c23	down	2.13	gi|114051229	Microtubule-associated protein RP/EB family member 3	5.48/6.27	31/29.98	9	37%	829	
c24	down	2.15	gi|291045214	Isopentenyl-diphosphate delta isomerase	6.37/6.57	30/27.16	8	31%	325	Hydrolase isopentenyl-diphosphate delta-isomerase activity, isoprenoid biosynthetic process
c25	down	2.53	gi|512892238	Carbonic anhydrase 2	5.92/6.41	31/27.45	5	28%	420	Carbonate dehydratase activity, one-carbon metabolic process
c26	down	2.32	gi|160333678	Glutathione S-transferase sigma 2	5.85/6.89	23/24.17	9	53%	864	Transferase activity
c27	down	4.37	gi|112982671	Ribosomal protein S12	5.79/6.21	15/15.97	6	75%	385	Structural constituent of ribosome, translation
c28	up	64.59	gi|49868	Beta-actin (aa 27-375) [Mus musculus]	5.78/6.13	39/32.55	5	19%	389	ATP binding, identical protein binding, kinesin binding, nitric-oxide-synthase binding, RNA polymerase II core promoter proximal region sequence-specific DNA binding
c29	up	72.24	gi|114051866	Isocitrate dehydrogenase	6.24/6.91	47/43.92	7	15%	329	Isocitrate dehydrogenase (NADP+) activity, magnesium ion binding, NAD binding, isocitrate metabolic process, tricarboxylic acid cycle
c30	**up**	**2.96**	**gi|153792114**	**Phosphatidylethanolamine-binding protein isoform 2**	**5.96/5.81**	**22/20.57**	**5**	**39%**	**230**	**Defence response to Gram-negative/positive bacteria, regulation of antimicrobial humoral response**
c31	up	9.61	gi|512902782	Uncharacterized protein LOC101738880 isoform X1	5.75/5.55	25/20.54	8	45%	791	
c32	up	4.1	gi|4574740	Tat-binding protein-1 [Drosophila melanogaster]	5.39/5.73	48.4/49.32	3	13%	277	ATPase activity, ATP binding, proteasome-activating ATPase activity, TBP-class protein binding
c33	up	4.88	gi|51555848	Glycerol-3-phosphate dehydrogenase-2	5.62/6.4	39/31.69	10	34%	850	Glycerol-3-phosphate dehydrogenase [NAD+] activity, NAD binding, carbohydrate metabolic process, glycerol-3-phosphate catabolic process
c34	up	2.53	gi|114053311	26S protease regulatory subunit 6B	5.09/5.61	47/50.98	6	17%	337	ATP binding, peptidase activity, protein catabolic process
c35	up	58.24	gi|347326520	DNA supercoiling factor	4.48/5.53	40/40.96	7	27%	476	Calcium ion binding

Spot no.[a]	BC9+ vs. BC9-[b]	Ratio[b]	Accession no.[c]	Protein name[c]	Theoretical/ Observed *PI*[d]	Theoretical/ Observed MW (kDa)[d]	Matched unique peptides[e]	Sequence coverage (%)[e]	Protein score[e]	Molecular/biological function[f]
c36	down	2.79	gi|512891246	Proteasome subunit alpha type-1 isoform X2	6.01/6.82	31/31.02	8	39%	516	Endopeptidase activity, threonine-type endopeptidase activity
c37	up	136.6	gi|512934137	Selenium-binding protein 1 isoform X2	5.68/6.42	53/52.96	5	15%	298	Selenium binding
c38	up	4.9	gi|512914963	Probable methylmalonate-semialdehyde dehydrogenase [acylating]	7.59/7.36	56/54.89	10	23%	758	Aldehyde dehydrogenase (NAD) activity, fatty-acyl-CoA binding, methylmalonate semialdehyde dehydrogenase (acylating) activity, thymine metabolic process, valine metabolic process
c39	up	10.69	gi|156255210	L-lactate dehydrogenase	6.76/7.72	37/33.93	3	9%	172	L-lactate dehydrogenase activity, carbohydrate metabolic process, carboxylic acid metabolic process

3. Mitochondrial proteins

2-DE images of mitochondrial protein extracts from P50 and BC9 following BmNPV infection.

14 DEPs with significant changes were selected for MALDI-TOF MS analysis.

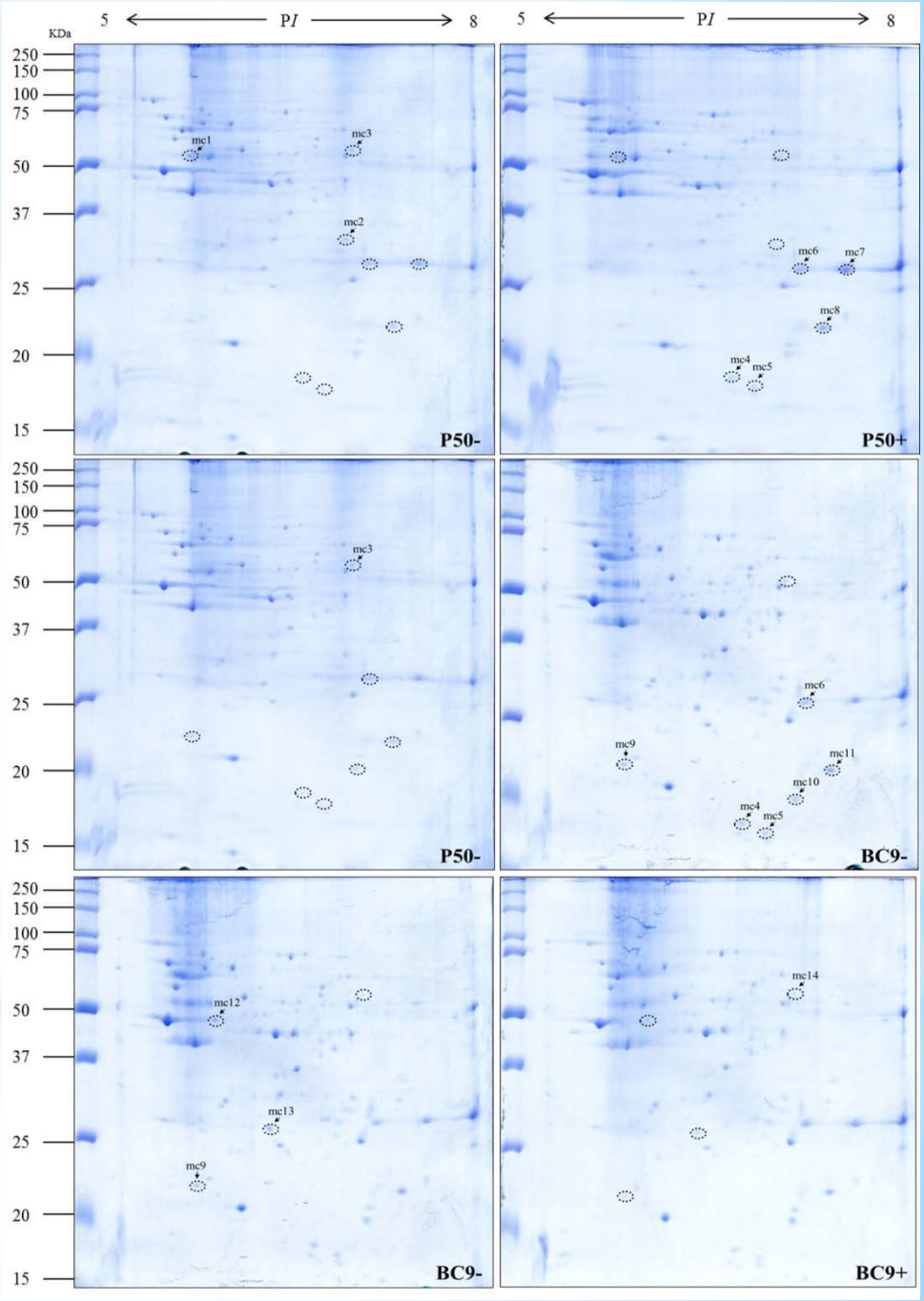

Identified proteins from mitochondrial fraction that changed significantly in different resistant strains following BmNPV infection.

Spot no.[a]	P50+ vs. P50-[b]	Ratio[b]	Accession no[c]	Protein name[c]	Theoretical/ Observed PI[d]	Theoretical/ Observed MW (kDa)[d]	Pep. Count[e]	Sequence coverage (%)[e]	Protein Score[e]	Molecular/biological function[f]
mc1	down	4.23	gi|62241292	Protein disulfide-isomerase	5.3/5.75	55.5/52.39	17		99.97	Protein disulfide isomerase activity, cell redox homeostasis
mc2	down	11.58	gi|336454478	Heat shock protein 70-3	5.12/6.9	72.8/30.53	17		100	ATP binding
mc3	down	6.31	gi|827547570	Dihydrolipoyllysine-residue succinyltransferase component of 2-oxoglutarate dehydrogenase complex	9.28/6.93	50.4/53.97	7	18%	361/58	Dihydrolipoyllysine-residue succinyltransferase activity, tricarboxylic acid cycle
mc4	up	12.41	gi|114052454	NADH dehydrogenase [ubiquinone] 1 beta subcomplex subunit 10	5.93/6.62	19.3/17.96	8	60%	521/58	Oxidation-reduction process
mc5	up	17.81	gi|512890394	Golgin subfamily A member 4	5.05/6.78	30.8/17.3	43		95.118	Protein targeting to Golgi
mc6	up	11.56	gi|512928976	Voltage-dependent anion-selective channel isoform X2	6.96/6.79	30.1/27.03	18		100	Voltage-gated anion channel activity
mc7	up	3.65	gi|512928976	Voltage-dependent anion-selective channel isoform X2	6.96/7.42	30.1/27.03	17		100	Voltage-gated anion channel activity
mc8	up	5.02	gi|98990259	Cytochrome b-c1 complex subunit Rieske	8.59/7.25	29.4/21.47	11		99.982	2 iron, 2 sulfur cluster binding, metal ion binding, ubiquinol-cytochrome-c reductase activity

Spot no.	BC9- vs. P50-[b]	Ratio[b]	Accession no.[c]	Protein name[c]	Theoretical/ Observed PI[d]	Theoretical/ Observed MW (kDa)[d]	Matched unique peptides[e]	Pep. Count[e]	PROTEIN score(%)[e]	Molecular/biological function[f]
mc9	**up**	**2.58**	**gi|87248369**	**NADH dehydrogenase (ubiquinone) Fe-S protein 8**	**6.15/5.79**	**25.5/21.83**	**13**		**100**	**4 iron, 4 sulfur cluster binding, oxidoreductase activity, acting on NAD(P)H**
mc10	up	3.86	gi|38260562	Thiol peroxiredoxin	6.09/7	22.07/19.63	10		100	Peroxiredoxin activity
mc11	up	3.62	gi|98990259	Cytochrome b-c1 complex subunit Rieske	8.59/7.25	29.4/21.47	11		99.982	2 iron, 2 sulfur cluster binding, metal ion binding, ubiquinol cytochrome c reductase activity
Spot no.[a]	BC9+ vs. BC9-[b]	Ratio[b]	Accession no.[c]	Protein name[c]	Theoretical/ Observed PI[d]	Theoretical/ Observed MW (kDa)[d]	Matched unique peptides[e]	Pep. Count[e]	Protein score(%)[e]	Molecular/biological function[f]
mc12	down	6.05	gi|95102940	H^+-transporting ATP synthase beta subunit isoform 2	5.32/5.92	54.9/47	15		99.488	ATP binding, proton-transporting ATP synthase activity
mc13	down	4.44	gi|87248085	Chaperonin-containing t-complex polypeptide 1 beta	6.32/6.96	58/55.19	18		100	ATP binding, protein folding
mc14	up	2.1	gi|512892238	Carbonic anhydrase 2	5.92/6.31	30.04/26.15	9		100	Carbonate dehydratase activity, one-carbon metabolic process

4. Microsomal proteins

2-DE images of microsomal protein extracts from P50 and BC9 following BmNPV infection.

35 DEPs with significant changes were selected for MALDI-TOF MS analysis.

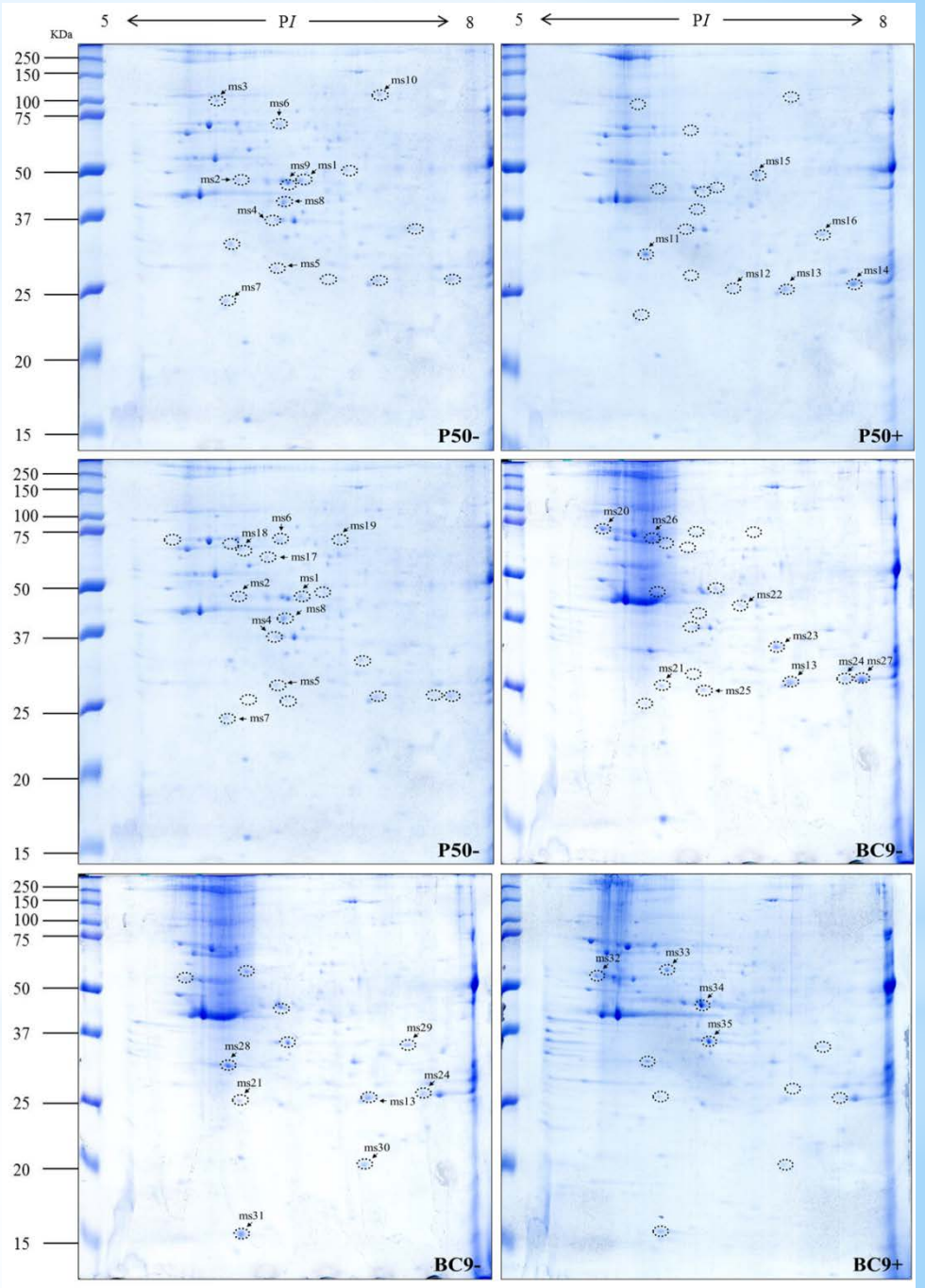

Identified proteins from microsomal fraction that changed significantly in different resistant strains following BmNPV infection.

Spot no.[a]	P50+ vs. P50-[b]	Ratio[b]	Accession no.[c]	Protein name[c]	Theoretical/ Observed PI[d]	Theoretical/ Observed MW (kDa)[d]	Matched unique peptides[e]	Sequence coverage (%)[e]	Protein score[e]	Molecular/biological function[f]
ms1	down	33.35	gi|148298800	Enolase	5.62/6.1	47/47.82	9	30%	795	Magnesium ion binding, phosphopyruvate hydratase complex, glycolytic process
ms2	down	27.28	gi|512913423	Uncharacterized protein LOC101745964	6.04/6.02	51/53	4	11%	193	
ms3	down	78.57	gi|112983322	Transitional endoplasmic reticulum ATPase TER94	5.3/5.94	90/101.55	8	15%	589	ATPase activity, hydrolase activity
ms4	down	48.18	gi|114051800	Eukaryotic translation initiation factor 3 subunit I	5.71/6.39	37/36.77	10	42%	707	Translation initiation factor activity, formation of translation preinitiation complex, regulation of translational initiation
ms5	down	13.14	gi|512892238	Carbonic anhydrase 2	5.92/6.39	31/28.44	4	22%	265	Carbonate dehydratase activity, one-carbon metabolic process
ms6	down	65.11	gi|512912927	Sorting nexin lst-4	5.61/6.4	64/71.17	9	17%	415	Phosphatidylinositol-3,4,5-trisphosphate binding, intracellular protein transport, phagosome-lysosome fusion involved in apoptotic cell clearance
ms7	down	15.99	gi|114053117	Eukaryotic translation initiation factor 3 subunit K	5.38/6	25/24.27	3	12%	170	Ribosome binding, translation initiation factor activity, formation of translation preinitiation complex, regulation of translational initiation
ms8	down	2.83	gi|112983906	Eukaryotic translation initiation factor 3 subunit H	5.68/5.92	39/54.61	5	16%	343	Translation initiation factor activity, formation of translation preinitiation complex
ms9	down	9.05	gi|112983898	Elongation factor 1 gamma	5.83/6.47	49/46.85	8	21%	587	Translation elongation factor activity
ms10	down	2.68	gi|112983010	Translation elongation factor 2 isoform 1	6.23/7.16	98/113.15	4	9%	223	GTPase activity, GTP binding, translation elongation factor activity
ms11	up	2.5	gi|827548126	Pyruvate dehydrogenase E1 component beta subunit isoform X1	6.03/6.04	40/32.43	10	35%	594	Pyruvate dehydrogenase (acetyl-transferring) activity, acetyl-CoA biosynthetic process from pyruvate
ms12	up	15.59	gi|87248109	Enoyl-CoA hydratase precursor 1	8.44/6.72	32/26.8	7	31%	452	Catalytic activity
ms13	up	9.14	gi|827537214	Probable enoyl-CoA hydratase, mitochondrial	9.28/7.14	32/26.74	10	42%	874	Catalytic activity
ms14	up	3.08	gi|827537214	Probable enoyl-CoA hydratase, mitochondrial	9.28/7.69	32/26.84	10	39%	896	Catalytic activity
ms15	up	2.09	gi|114052278	ATP synthase	9.21/6.91	60/51.66	4	5%	128	ATP binding, proton-transporting ATPase activity, proton-transporting ATP synthase activity
ms16	up	3.87	gi|153792309	Pyruvate dehydrogenase	8.07/7.43	44/34.96	8	27%	410	Pyruvate dehydrogenase (acetyl-transferring) activity, glycolytic process

Spot no.[a]	BC9- vs. P50-[b]	Ratio[b]	Accession no.[c]	Protein name[c]	Theoretical/ Observed PI[d]	Theoretical/ Observed MW (kDa)[d]	Matched unique peptides[e]	Sequence coverage (%)[e]	Protein score[e]	Molecular/biological function[f]
ms17	down	99.96	gi|512903088	Mitochondrial import receptor subunit Tom70	5.55/6.31	62/62.95	8	16%	391	Receptor
ms18	down	5.77	gi|512899307	Esterase FE4-like	5.27/6.12	68/66.96	5	5%	206	Hydrolase activity
ms19	down	64.93	gi|112983574	Carboxylic ester hydrolase	7.09/6.85	55/71.74	6	16%	217	Hydrolase activity
ms20	up	166.38	gi|336454478	Heat shock protein 70-3	5.12/5.59	73/71.7	10	21%	647	ATP binding
ms21	**up**	**65.6**	**gi|304307739**	**Tudor staphylococcus/micrococcal nuclease**	**8.56/6.12**	**99/26.35**	**9**	**13%**	**664**	**Transcription cofactor activity, posttranscriptional gene silencing by RNA**
ms22	up	38.05	gi|112983926	Arginine kinase	5.87/6.75	40/42.06	9	32%	561	ATP binding, kinase activity,
ms23	up	33.53	gi|124245114	Glucose-regulated protein 78 [Fenneropenaeus chinensis]	5.00/6.74	72.8/48.85	5	11%	491	ATP binding, Nucleotide-binding
ms24	up	34.91	gi|112982960	Ferritin precursor	6.75/7.56	26/26.95	4	31%	441	Ferric iron binding, ferroxidase activity, cellular iron ion homeostasis, iron ion transport
ms25	up	8	gi|153792257	Trypsin-like protease	5.62/6.5	28/25.84	3	17%	184	Serine-type endopeptidase activity
ms26	up	10.16	gi|5751	Actin a3	5.47/6.05	42/68.45	4	12%	238	ATP binding
ms27	up	2.5	gi|827537214	Probable enoyl-CoA hydratase, mitochondrial	9.28/7.69	32/26.84	10	39%	893	Catalytic activity
Spot no.[a]	BC9+ vs. BC9-[b]	Ratio[b]	Accession no.[c]	Protein name[c]	Theoretical/ Observed PI[d]	Theoretical/ Observed MW (kDa)[d]	Matched unique peptides[e]	Sequence coverage (%)[e]	Protein score[e]	Molecular/biological function[f]
ms28	down	2.06	gi|827548126	Pyruvate dehydrogenase e1 component beta subunit isoform x1	6.03/6.04	40/32.43	10	35%	625	Pyruvate dehydrogenase (acetyl-transferring) activity, acetyl-CoA biosynthetic process from pyruvate
ms29	down	6.04	gi|32400724	Alpha-tubulin [oikopleura dioica]	4.94/5.64	51/55.62	9	31%	805	GTPase activity, GTP binding, structural constituent of cytoskeleton
ms30	down	2.76	gi|148298878	Vacuolar ATP synthase catalytic subunit a	5.27/6.18	69/58.88	9	16%	622	ATP binding, proton-transporting ATPase activity, ATP hydrolysis-coupled proton transport, ATP metabolic process
ms31	down	2.3	gi|15213812	Ribosomal protein s12 [spodoptera frugiperda]	5.79/6.17	15/15.67	6	62%	542	Structural constituent of ribosome, translation
ms32	up	198.68	gi|153092309	Pyruvate dehydrogenase	8.07/7.43	44/34.96	9	28%	511	Pyruvate dehydrogenase (acetyl-transferring) activity, glycolytic process
ms33	up	2.47	gi|112982996	Thiol peroxiredoxin	6.09/7.13	22/20.17	6	37%	456	Peroxiredoxin activity
ms34	up	5.79	gi|112983898	Elongation factor 1 gamma	5.83/6.48	49/46.85	10	26%	704	Translation elongation factor activity
ms35	up	3.4	gi|114051800	Eukaryotic translation initiation factor 3 subunit Ⅰ	5.71/6.52	37/36.46	10	32%	672	Translation initiation factor activity, formation of translation preinitiation complex, regulation of translational initiation

5. KEGG pathway classification analysis of the DEPs in each subcellular fractions.

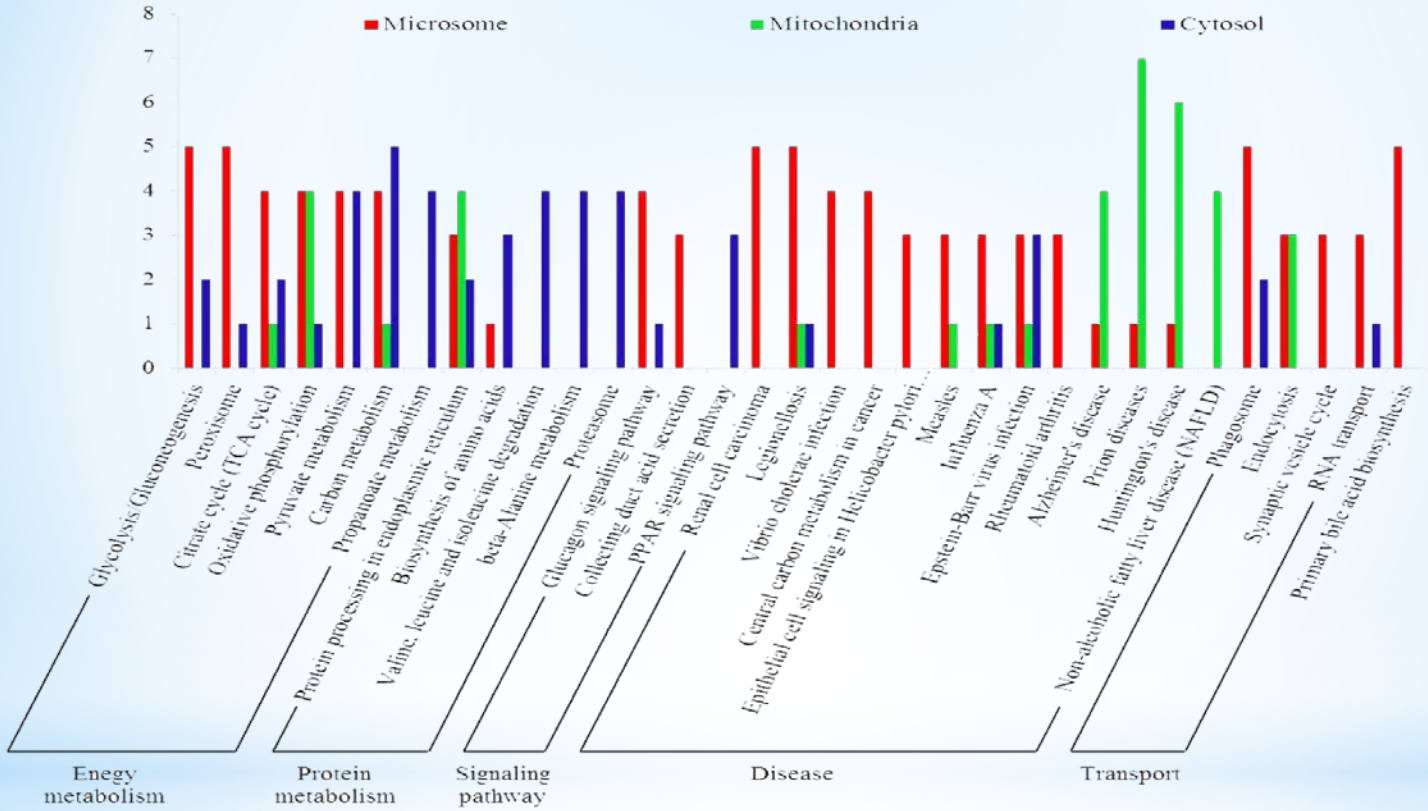

Among the 87 identified DEPs, 63 proteins were involved in specific KEGG pathways. The relevant pathways were classified into five main categories and 33 subcategories according to the KEGG classifications.

在Microsome，这些差异表达蛋白主要参与了energy metabolism (28%)，disease (39%)和transport (15%)。在Mitochondria中（绿色），差异表达蛋白主要参与了energy metabolism (16%)和disease (66%)。在Cytosol中（蓝色），差异表达蛋白主要参与了energy metabolism (40%) 和 protein metabolism (35%)。

6. DEPs in three subcellular fractions of different resistant strains following BmNPV infection.

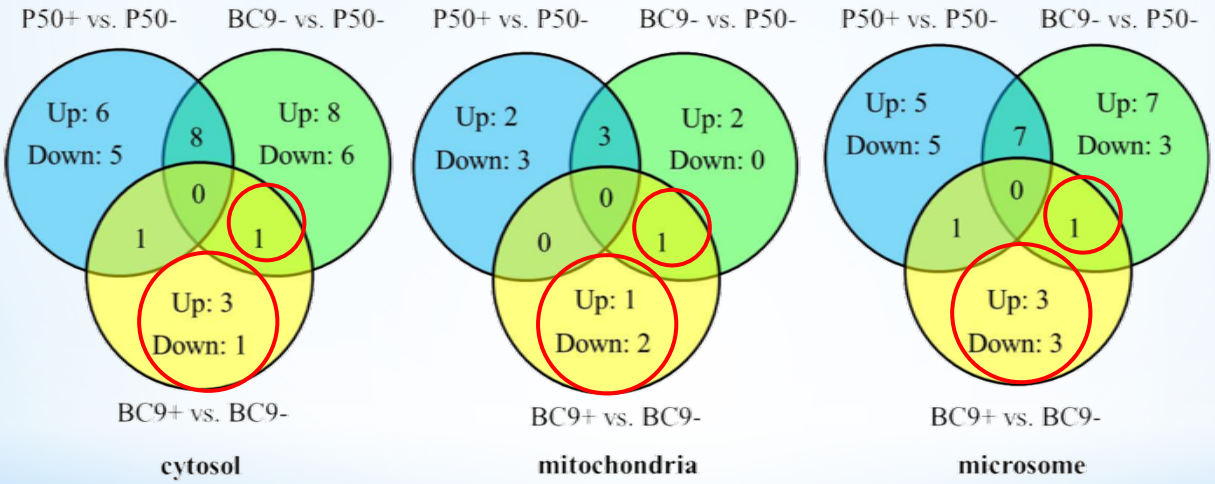

After removing DEPs relevant to the genetic background and immune stress response, 16 proteins (region of yellow colour) that were uniquely differentially expressed in BC9 following infection were obtained, which were potentially involved in the BmNPV-stimulated or pathologic response.

7. The interaction network of 16 DEPs of interest was constructed based on the STRING website information using the database of *D. melanogaster*.

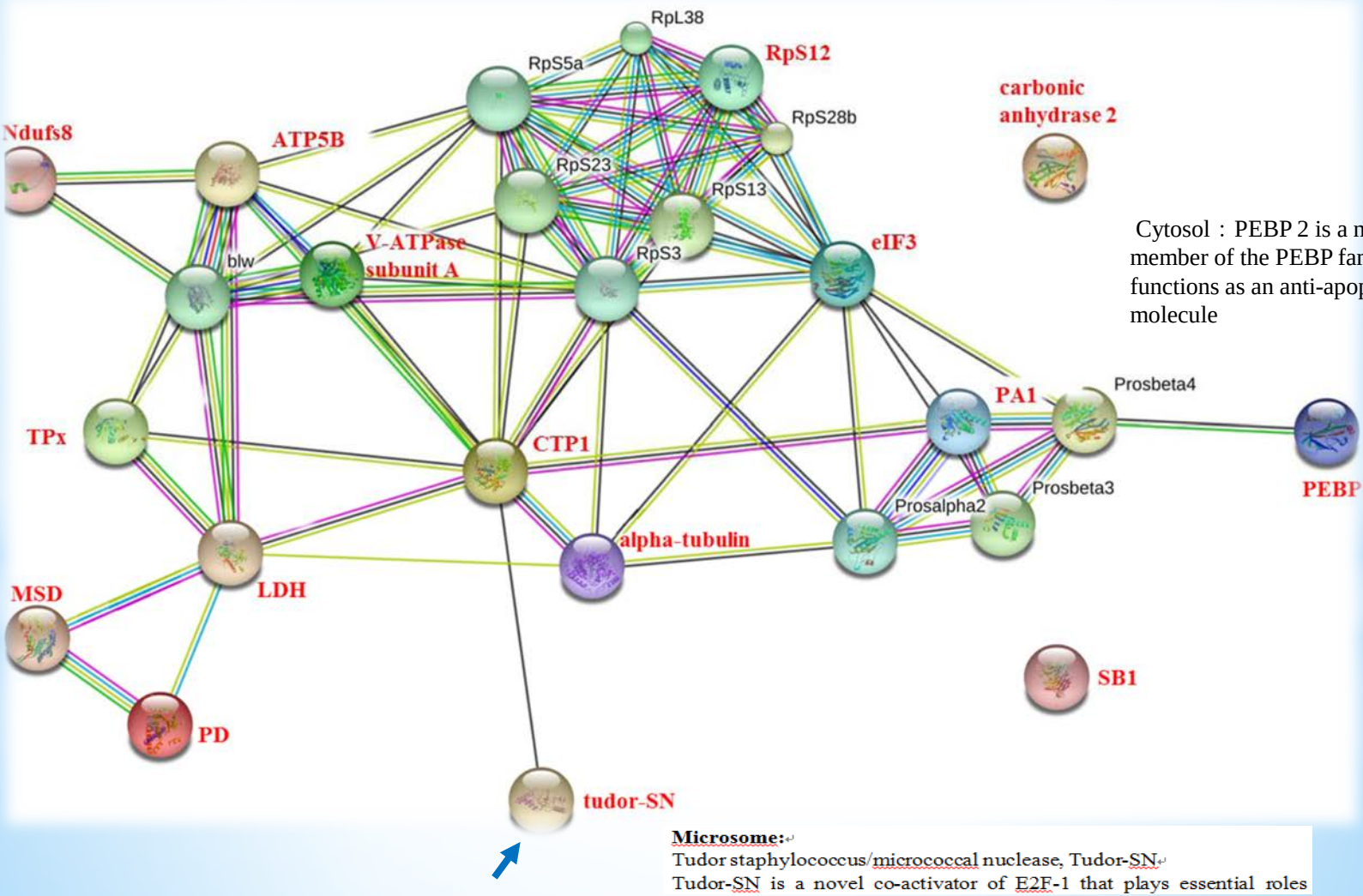

Cytosol：PEBP 2 is a novel member of the PEBP family and functions as an anti-apoptotic molecule

Microsome:
Tudor staphylococcus/micrococcal nuclease, Tudor-SN
Tudor-SN is a novel co-activator of E2F-1 that plays essential roles

Enlarged spot images and RT-qPCR analysis of the expression levels of anti-BmNPV-relevant DEPs.

Eight proteins exhibited highly similar differential expression patterns at the translational and transcriptional levels in BC9 following infection. Additionally, nearly all of these proteins exhibited significant differences in expression in BC9 following infection.

Cytosol: Phosphatidylethanolamine-binding protein isoform 2, it is a novel member of the PEBP family and functions as an anti-apoptotic molecule. In our study, the expression levels of TPx and PEBP in BC9 following BmNPV infection were significantly down-regulated, without notable changes in P50.

Mitochondria: NADH dehydrogenase (ubiquinone) Fe-S protein 8 , Ndufs8 is a subunit of mitochondrial NADH, which is primarily involved in the binding of two of the six to eight iron-sulfur clusters of a complex. It is reported that Ndufs8 is down-regulated in mice with hyperhomocysteinaemia (HHcy) disease and is involved in energy metabolism.

Microsome: Tudor staphylococcus/micrococcal nuclease, Tudor-SN is a novel co-activator of E2F-1 that plays essential roles in the G1/S transition during cellular division. An analysis of intracellular antigens revealed the presence of reovirus in dividing but not quiescent hepatocytes, indicating that cellular division could promote virus replication.


Thanks for your Attention!